
Multi-dimensional Tensor Sketch: Dimensionality Reduction That Retains Efficient Tensor Operations

Yang Shi¹ Animashree Anandkumar²

Abstract

Sketching refers to a class of randomized dimensionality reduction methods that aim to preserve relevant information in large-scale datasets. They have efficient memory requirements and typically require just a single pass over the dataset. Efficient sketching methods have been derived for vector and matrix-valued datasets. When the datasets are higher-order tensors, a naive approach is to flatten the tensors into vectors or matrices and then sketch them. However, this is inefficient since it ignores the multi-dimensional nature of tensors. In this paper, we propose a novel multi-dimensional tensor sketch (MTS) that preserves higher order data structures while reducing dimensionality. We build this as an extension to the popular count sketch (CS) and show that it yields an unbiased estimator of the original tensor. We demonstrate significant advantages in compression ratios when the original data has decomposable tensor representations such as the Tucker, CP, tensor train or Kronecker product forms. We apply MTS to tensorized neural networks where we replace fully connected layers with tensor operations. We achieve nearly state of art accuracy with significant compression on image classification benchmarks.

1. Introduction

Many modern machine learning and data mining applications involve manipulating large-scale multi-dimensional data structures. For instance, the input data can be multi-modal or multi-relational (e.g. combination of image and text), and the intermediate computations can involve higher-order tensor operations (e.g. layers in a tensorized neural network). Memory, bandwidth and computational requirements are usually bottlenecks when these operations are done at scale. Efficient dimensionality reduction schemes

can greatly alleviate this issue if they can find a compact representation while preserving accuracy.

A popular class of dimensionality reduction techniques involve spectral decomposition, such as principle component analysis (PCA), singular value decomposition (SVD) and tensor decompositions. They aim to fit the datasets using low rank approximations, which can be interpreted as a low-dimensional latent structure in the data. They have shown good performance in many applications such as topic modelling (Aza et al., 2001) and recommendation systems (Koren et al., 2009). However, for large-scale datasets, exact computation of spectral decompositions is expensive and randomized methods are used instead.

Sketching forms another class of randomized dimensionality reduction methods. These methods have efficient memory requirements and typically do just a single pass on the data. They have approximation guarantees in recovering the original data. In addition, they allow for certain operations to be accurately carried out in the low-dimensional sketched space, e.g. inner products and outer products on vectors. Count sketch (CS) is the simplest sketching technique (Charikar et al., 2002) that uses random signs and random hash functions to carry out dimensionality reduction. This has been applied in many settings. Demaine et al. (2002) design a frequency estimation of internet packet streams. The purpose is to determine essential features of the traffic stream using limited space. Another application is multi-modal pooling of features, e.g. in visual question and answering (VQA), this involves bilinear pooling of image and text features.

Sketching techniques, however, mostly focus on vector and matrix-valued data. A few works attempt to extend to higher order tensors: e.g. to non-linear kernels (Pham & Pagh, 2013) and to higher order tensors (Wang et al., 2015), which we refer to as Count-based Tensor Sketch (CTS). However, they view the tensor as sets of vectors and sketch along each fibre¹ of the tensor. Hence, they still use inherently vector-based sketching techniques and do not exploit the complete multi-dimensional nature of data, and can miss correlations across different modes. For instance, the image feature

¹University of California, Irvine, USA ²California Institute of Technology, USA. Correspondence to: Yang Shi <shiy4@uci.edu>.

¹Fibre is the higher order analogue of matrix rows and columns.

extracted from the traditional vision network contains spatial information. Separating these data at each location ignores the connection between adjacent pixels.

Main contributions: We propose multi-dimensional tensor sketch (MTS), which is the first method to fully exploit the multi-dimensional nature of higher order tensors. It projects the original tensor to another tensor, which can be of the same order, but with smaller dimensions (which affect the recovery guarantees). This allow for efficient computation of various operations such as tensor product and tensor contractions by directly applying operations on the sketched components. MTS has advantages over vector-based sketching methods such as CTS when the underlying tensor has special forms such as Kronecker product, Tucker-form, CP-form or tensor-train forms. Computation and memory improvement over CTS is summarized in Table 1.

We compare MTS and CTS for Kronecker product compression using synthetic data. MTS outperforms CTS in aspect of relative error while using $10\times$ less computation time when they keep the same compression ratio. We apply MTS for approximating tensor operations in tensorized neural networks. These networks replace fully connected layers with multi-linear tensor algebraic operations. This results in compression since multi-linear layers can take better advantage of spatial information available in activations from convolutional layers. Applying MTS to tensor operations further results in compression while preserving accuracy. We demonstrate efficiency on CIFAR10 dataset.

Table 1: Ratio of improvement using MTS over CTS on different tensor operations. (Assume input for Kronecker product is a n -dimension square matrix, input for tensor contraction is a third-order tensor with dimension n and rank r)

Operator	Computation	Memory
Kronecker Product	$O(n)$	$O(n^2)$
Tucker-form Tensor	$O(r^2)$ if $r^3 < n$, $O(r^3)$ if $r^3 > n$	$O(r)$
CP-form Tensor	$O(r)$ if $r > n$	$O(r)$
Tensor-train	$O(r^2)$ if $\log r > n$	$O(n)$

Important Tensor Applications: We focus on tensor sketching because data is inherently multi-dimensional. In probabilistic model analysis, tensor decomposition is the crux of model estimation via the method of moments. A variety of models such as topic models, hidden Markov models, Gaussian mixtures etc., can be efficiently solved via the tensor decomposition techniques under certain mild assumptions (Anandkumar et al., 2014). Tensor methods are also relevant in deep learning. Yu et al. learn the nonlinear dynamics in recurrent neural networks directly using higher order state transition functions through tensor train decomposition. Kossaifi et al. (2017) propose tensor contraction and regression layers in deep convolutional neural networks.

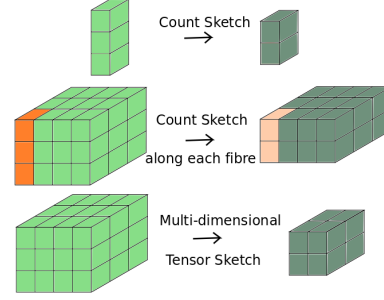


Figure 1: Multi-dimensional tensor sketch of a third-order tensor.

Table 2: Summary of notations.

Notation	Meaning
$\text{FFT}(a)$	1D Fourier Transform
$\text{IFFT}(a)$	1D Inverse Fourier Transform
$a \circ b$	Element-wise Product
$a * b$	Convolution
$A \otimes B$	Kronecker Product
$\text{FFT2}(A)$	2D Fourier Transform
$\text{IFFT2}(A)$	2D Inverse Fourier Transform
A^{-1}	Matrix Inverse
\hat{A}	Decompression
$[n]$	$\{1, 2, \dots, n\}$

Instead of mapping high-order activation tensor to vectors to pass through a fully connected layer, they generate tensor weights to filter the multi-dimensional activation tensor. Tensor product is used in combining different features in multi-modal tasks. Visual Question Answering task (Antol et al., 2015) requires integration of feature maps from image and text that have drastically different structures. Many studies have been done to explore various features and combine them wisely based on their structures (Fukui et al., 2016; Teney et al., 2017; Shi et al., 2018).

2. Multi-dimensional Tensor Sketch

In this section, we first present important definitions and theorems in previous literature. We then define the multi-dimensional tensor sketch and present its approximation guarantees. We show the superiority of this sketch, comparing to CS, in approximating Kronecker product.

2.1. Tensor

We denote vectors by lowercase letters, matrices by uppercase letters, higher-order tensors (multi-dimensional data structures) by calligraphic uppercase letters. The order of a tensor is the number of modes it admits. For example, $\mathcal{T} \in \mathbb{R}^{n_1 \times \dots \times n_N}$ is a N th-order tensor because it has N modes. A scalar is a zeroth-order tensor, a vector is a first-

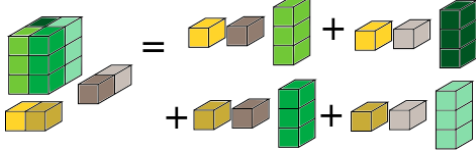


Figure 2: Tensor contraction example: given $\mathcal{A} \in \mathbb{R}^{2 \times 2 \times 3}$, $u \in \mathbb{R}^{2 \times 1}$, $v \in \mathbb{R}^{2 \times 1}$, $\mathcal{A}(u, v, I) \in \mathbb{R}^{1 \times 1 \times 3}$ ($I \in \mathbb{R}^{3 \times 3}$ is an identity matrix).

order tensor, a matrix is a second-order tensor with the rows being the first mode and columns being the second mode, and a three-way array (say $\mathcal{A} \in \mathbb{R}^{m \times n \times p}$) is a third-order tensor with the first, second and third modes indexed by m , n , and p , respectively.

Tensor product is known as outer product in vectors case. A N th-order tensor is an element of the tensor product of N vector spaces: $\mathcal{A} = v_1 \otimes \cdots \otimes v_N \in \mathbb{R}^{n_1 \times \cdots \times n_N}$, where $v_i \in \mathbb{R}^{n_i}$, $i \in 1, \dots, N$. Assume $V_i \in \mathbb{R}^{n_i \times m_i}$, $i \in 1, \dots, N$, **tensor contraction** $\mathcal{A}(V_1, \dots, V_N) \in \mathbb{R}^{m_1 \times \cdots \times m_N}$, and element-wise:

$$\mathcal{A}(V_1, \dots, V_N)_{i_1, \dots, i_N} = \sum_{j_1, \dots, j_N} \mathcal{A}_{j_1, \dots, j_N} V_{1j_1, i_1} \cdots V_{Nj_N, i_N}$$

We show a tensor contraction example in Figure 2. **Tensor decomposition** is an extension of matrix decomposition to higher orders. The Tucker decomposition (Tucker, 1966) is analogous to principal component analysis. It decomposes a tensor as a core tensor contracted with a matrix along each mode. For instance, a third-order tensor $\mathcal{T} \in \mathbb{R}^{n_1 \times n_2 \times n_3}$ has Tucker decomposition:

$$\mathcal{T} = \mathcal{G}(U, V, W) \quad (1)$$

where $\mathcal{G} \in \mathbb{R}^{r_1 \times r_2 \times r_3}$, $U \in \mathbb{R}^{n_1 \times r_1}$, $V \in \mathbb{R}^{n_2 \times r_2}$, $W \in \mathbb{R}^{n_3 \times r_3}$. CANDECOMP/PARAFAC(CP) (Harshman, 1970) is a special case of Tucker-form tensor: the core tensor is a sparse tensor that only diagonal data have non-zero values. It can be represented as a sum of rank-1 tensors. In previous example, $\mathcal{T} = \sum_{i=1}^r \mathcal{G}_{iii} U_i \otimes V_i \otimes W_i$. Figure 3 shows the Tucker-form and CP-form of a third-order tensor. By splitting variables, Tensor Train (TT) (Oseledets, 2011) can represent a high order tensor with several third order tensors.

2.2. Count Sketch

We describe Count Sketch(CS) in Algorithm 1. The estimation can be made more robust by taking d independent sketches of the input and calculate the median of the d estimators. Charikar et al. (2002) prove that the CS is an unbiased estimator with variance bounded by the 2-norm of the input. Pagh (2012) use CS and propose a fast algorithm to compute count sketch of an outer product of two vectors.

$$CS(u \otimes v) = CS(u) * CS(v) \quad (2)$$

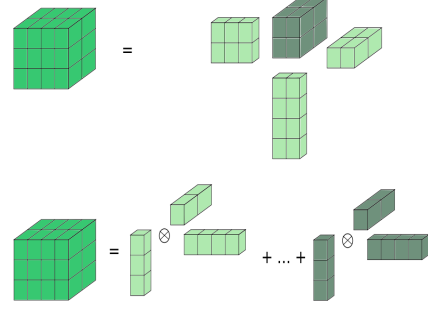


Figure 3: Tucker(upper) and CP(lower) decomposition of a third-order tensor.

The convolution operation can be transferred to element-wise product using FFT properties. Thus, the computation complexity reduces from $O(n^2)$ to $O(n + c \log c)$, if the vectors are of size n and the sketching size is c .

Notice that CS can be applied to each fibre of the input tensor, we can always sketch a tensor using CS. We call this Count-based Tensor Sketch(CTS). Algorithm 2 describes the CTS. The disadvantage is the ignorance of the connections between fibres, as we mentioned in Section 1.

2.3. Proposed: Multi-dimensional Tensor Sketch(MTS)

Given a tensor $\mathcal{T} \in \mathbb{R}^{n_1 \times \cdots \times n_N}$, random hash functions $h_1: [n_1] \rightarrow [m_1], \dots, h_N: [n_N] \rightarrow [m_N]$, and random sign functions $s_1: [n_1] \rightarrow \{\pm 1\}, \dots, s_N: [n_N] \rightarrow \{\pm 1\}$:

$$MTS(\mathcal{T})_{t_1, \dots, t_N} = \sum_{h_1(i_1)=t_1, \dots, h_N(i_N)=t_N} s_1(i_1) \cdots s_N(i_N) \mathcal{T}_{i_1, \dots, i_N}$$

We can write the MTS using tensor operations.

$$MTS(\mathcal{T}) = (\mathcal{S} \circ \mathcal{T})(H_1, \dots, H_N) \quad (3)$$

Here $\mathcal{S} = s_1 \otimes \cdots \otimes s_N \in \mathbb{R}^{n_1 \times \cdots \times n_N}$, $H_i \in \mathbb{R}^{n_i \times m_i}$, $H_i(a, b) = 1$ if $h_i(a) = b$, for $\forall a \in [n_i]$, otherwise $H_i(a, b) = 0$. $MTS(\mathcal{T}) \in \mathbb{R}^{m_1 \times \cdots \times m_N}$ equals the signed tensor $(\mathcal{S} \circ \mathcal{T})$ contract with the hash matrices $(H_i, \text{ for } i \in [N])$ along each mode. To recover the original tensor, we have

$$\hat{\mathcal{T}}_{i_1, \dots, i_N} = s_1(i_1) \cdots s_N(i_N) MTS(\mathcal{T})_{h_1(i_1), \dots, h_N(i_N)}$$

, or in compact format

$$\hat{\mathcal{T}} = (\mathcal{S} \circ MTS(\mathcal{T}))(H_1^{-1}, \dots, H_N^{-1}) \quad (4)$$

We show MTS in Algorithm 3. We prove that this MTS is unbiased and it has variance of roughly $\|\mathcal{T}\|_F$. All detailed proofs are in Appendix B.2.

Theorem 2.1 (MTS recovery analysis). Given a tensor $\mathcal{T} \in \mathbb{R}^{n_1 \times \cdots \times n_N}$, MTS hash functions s_k, h_k with sketching dimensions m_k , for $k \in [N]$, the decompress Equation 4

Algorithm 1 Count Sketch (Charikar et al., 2002)

```

1: procedure CS( $x, c$ )  $\triangleright x \in \mathbb{R}^n$ 
2:    $s \in \text{Maps}([n] \Rightarrow \{-1, +1\})$ 
3:    $h \in \text{Maps}([n] \Rightarrow \{0, \dots, c\})$ 
4:   for  $i:1$  to  $n$  do
5:      $y[h[i]] += s[i]x[i]$ 
6:   return  $y$ 
7: procedure CS-DECOMPRESS( $y$ )
8:   for  $i:1$  to  $n$  do
9:      $\hat{x}[i] = s[i]y[h[i]]$ 
10:  return  $\hat{x}$ 

```

Algorithm 2 Count-based Tensor Sketch

```

1: procedure CTS( $\mathcal{T}, c$ )  $\triangleright \mathcal{T} \in \mathbb{R}^{n_1 \times \dots \times n_N}$ 
2:   for each fibre  $x$  in  $\mathcal{T}$  do
3:     each fibre in  $CTS(\mathcal{T}) = CS(x, c)$ 
4:   return  $CTS(\mathcal{T})$ 
5: procedure CTS-DECOMPRESS( $CTS(\mathcal{T})$ )
6:   for each fibre  $x$  in  $CTS(\mathcal{T})$  do
7:     each fibre in  $\hat{\mathcal{T}} = CS\text{-Decompress}(x)$ 
8:   return  $\hat{\mathcal{T}}$ 

```

computes an unbiased estimator for $\mathcal{T}_{i_1^* \dots i_N^*}$ with variance bounded by $\|\mathcal{T}\|_F^2 / (m_1 \dots m_N)$, for any i_1^*, \dots, i_N^* .

In computational analysis, we assume $MTS(\mathcal{T})$ takes $O(n_1 \dots n_N)$ operations if $\mathcal{T} \in \mathbb{R}^{n_1 \times \dots \times n_N}$. However, we need to compute Equation 3 in a sequential way in practise. It requires extra permutations and copies without computation optimization. For example, given $\mathcal{T} \in \mathbb{R}^{n_1 \times n_2 \times n_3}$, $H_2 \in \mathbb{R}^{n_2 \times m_2}$, $\mathcal{T}(I, H_2, I)$ can be computed in three steps:

- reshape $\mathcal{T} \in \mathbb{R}^{n_1 \times n_2 \times n_3}$ to $\mathcal{T} \in \mathbb{R}^{n_1 n_3 \times n_2}$
- compute $\mathcal{P} = \mathcal{T}H_2 \in \mathbb{R}^{n_1 n_3 \times m_2}$
- reshape $\mathcal{P} \in \mathbb{R}^{n_1 n_3 \times m_2}$ to $\mathcal{P} \in \mathbb{R}^{n_1 \times m_2 \times n_3}$

Shi et al. (2016) propose a parallel computing scheme for tensor contraction using Basic Linear Algebra Subroutines (BLAS). Based on that, $\mathcal{T}(I, H_2, I)$ can be computed in one step without permutations:

- parallel compute n_3 number of matrix matrix multiplications: $\mathcal{P}_{:, :, i} = \mathcal{T}_{:, :, i} H_2, i \in [n_3]$

Recently released High-Performance Tensor Transposition (HPTT) is an open-source library that performs efficient tensor contractions (Springer et al., 2017). By applying these tensor contraction primitives, we can accelerate the sketching process in practise.

Algorithm 3 Multi-dimensional Tensor Sketch

```

1: procedure MTS( $\mathcal{T}, M_{list}$ )  $\triangleright \mathcal{T} \in \mathbb{R}^{n_1 \times \dots \times n_N}$ 
2:    $\triangleright M_{list}$  contains sketching parameters
3:   Generate hash functions  $s_1, \dots, s_N, h_1, \dots, h_N$ 
   given  $M_{list}$ 
4:   Compute hash matrices  $\mathcal{S}, H_1, \dots, H_N$ 
5:   return  $(\mathcal{S} \circ \mathcal{T})(H_1, \dots, H_N)$ 
6: procedure MTS-DECOMPRESS( $MTS(\mathcal{T})$ )
7:   return  $(\mathcal{S} \circ MTS(\mathcal{T}))(H_1^{-1}, \dots, H_N^{-1})$ 

```

2.4. Example: Approximate Kronecker Product

Pagh (2012) shows that the count sketch of an outer product equals the convolution between the count sketch of each input vector. Furthermore, the convolution operation in time domain can be transferred to element-wise product in frequency domain. Kronecker product is a generalization of outer product from vector to matrix. It is one kind of tensor product. Usually, the computation and memory cost are expensive as shown in Figure 4.

Sketching a Kronecker product using count-based tensor sketch (CTS) We compute the sketch of $A \otimes B$ by sketching each of the outer product(row-wise) using CTS. Assume $A, B \in \mathbb{R}^{n \times n}$, each outer product has $O(n + c \log c)$ operations and there are $O(n^2)$ such outer products. Thus, it requires a total $O(n^3 + n^2 c \log c)$ operations to sketch the Kronecker product.

Sketching a Kronecker product using multidimensional tensor sketch (MTS) We show that

$$MTS(A \otimes B) = MTS(A) * MTS(B) \quad (5)$$

Convolution in Equation 5 can be further simplified by converting sketched components to 2D-frequency domain. Assume $A' = MTS(A), B' = MTS(B)$:

$$FFT2(A' * B') = FFT2(A') \circ FFT2(B') \quad (6)$$

This approximation requires $O(n^2)$ to complete $MTS(A)$, $MTS(B)$ and $O(m^2 \log m)$ to complete 2D Fourier Transform if the MTS sketching parameter is m . The proof for Equation 5 is in Appendix B.1. This example shows the advantage of MTS in estimating tensor operations by directly applying operations on the sketched components. See Figure 5, 6 and Table 3 for comparison.

3. Sketched Tensor Representations

In this section, we discuss how to approximate tensors given different tensor representations: Tucker-form tensor, CP-form tensor and Tensor-train. We show that MTS is more efficient for compressing tensors given these forms compared to CTS, especially when the tensors are high-rank.

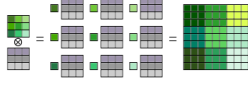


Figure 4: Kronecker product of two matrices with size $n \times n$. It requires $O(n^4)$ computation.



Figure 5: CTS of Kronecker product. It requires $O(n^2(n + c \log c))$ computations.

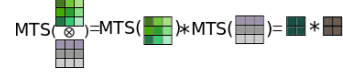


Figure 6: MTS of Kronecker product. It requires $O(n^2 + m^2 \log m)$ computations.

Table 3: Computation analysis of sketched Kronecker product using MTS and CTS (We choose $O(m^2) = O(c)$ to maintain same recovery error).

Operator	Computation
$CS(u \otimes v)$	$O(n + c \log c)$
$CTS(A \otimes B)$	$O(n^2(n + c \log c))$
$MTS(A \otimes B)$	$O(n^2 + c \log c)$

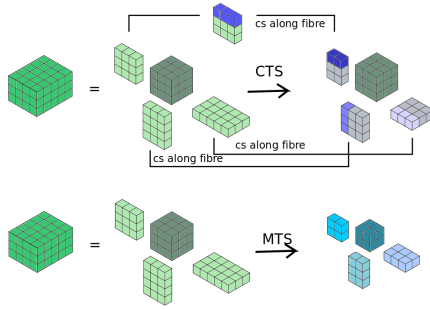


Figure 7: Sketch of a third-order Tucker-form tensor.

3.1. Tucker-form Tensor Sketching: CTS vs. MTS

The Tucker decomposition is a form of higher-order PCA. In the following analysis, we use a third-order tensor as an example. Define a tensor $\mathcal{T} \in \mathbb{R}^{n_1 \times n_2 \times n_3}$: $\mathcal{T} = \mathcal{G}(U, V, W)$. Here, $U \in \mathbb{R}^{n_1 \times r_1}$, $V \in \mathbb{R}^{n_2 \times r_2}$, $W \in \mathbb{R}^{n_3 \times r_3}$, $\mathcal{G} \in \mathbb{R}^{r_1 \times r_2 \times r_3}$. To simplify the analysis, we assume $r_1 = r_2 = r_3 = r$, $n_1 = n_2 = n_3 = n$. Figure 7 shows the difference between sketching methods using CTS and MTS.

3.1.1. CTS OF TUCKER-FORM TENSOR

To apply count sketch to the Tucker-form tensor, we rewrite the decomposition as a sum of rank-1 tensors. The CTS representation is:

$$\begin{aligned}
 CTS(\mathcal{T}) &= \sum_{a=1}^r \sum_{b=1}^r \sum_{c=1}^r \mathcal{G}_{abc} CS(U_a \otimes V_b \otimes W_c) \quad (7) \\
 &= \sum_{a=1}^r \sum_{b=1}^r \sum_{c=1}^r \mathcal{G}_{abc} CS(U_a) * CS(V_b) * CS(W_c)
 \end{aligned}$$

where U_a, V_b, W_c are a^{th}, b^{th}, c^{th} column of U, V, W respectively. \otimes is the tensor product (outer product in vector space). In this way, we can apply outer product sketching (Pagh, 2012) to each term in the summation. Notice that the convolution operation in Equation 7 can be computed through FFT. The computation complexity of this estimation process is $O(r^3(n + c \log c))$. The memory complexity is $O(rc + r^3)$.

Suppose $\hat{\mathcal{T}}$ is the recovered tensor for $\mathcal{T} = \mathcal{G}(U, V, W)$ after applying count sketch on U, V and W with sketching dimension c , $g = \|\mathcal{G}\|_{\max}$, $g_1 = \max(\|U_i\|_2)$, $g_2 = \max(\|V_j\|_2)$, $g_3 = \max(\|W_k\|_2)$ for $i \in [r], j \in [r], k \in [r]$. Suppose the estimation takes d independent sketches of U, V and W and then report the median of the d estimates:

Theorem 3.1 (CTS recovery analysis for Tucker tensor).

If $d = \Omega(\log(1/\delta))$, $c = \Omega(\frac{r^3 g g_1^2 g_2^2 g_3^2}{\epsilon^2})$, then with probability $\geq 1 - \delta$ there is $|\hat{\mathcal{T}}_{ijk} - \mathcal{T}_{ijk}| \leq \epsilon$.

Theorem 3.1 shows that the sketch length c can be set as $O(r^3)$ to provably approximate a 3rd-order Tucker-form tensor with dimension n , rank r .

3.1.2. MTS OF TUCKER-FORM TENSOR

The MTS of Tucker-form tensor can be done by MTS each of the factors and the core tensor. We rewrite $\mathcal{T} = (U \otimes V \otimes W)vec(\mathcal{G})$. Thus,

$$\begin{aligned}
 MTS(\mathcal{T}) &= MTS((U \otimes V \otimes W)vec(\mathcal{G})) \quad (8) \\
 &= \sum_{i=1}^{m_2} MTS((U \otimes V \otimes W)_i \otimes vec(\mathcal{G})_i) \\
 &= \sum_{i=1}^{m_2} MTS(U \otimes V \otimes W)_i * MTS(vec(\mathcal{G}))_i
 \end{aligned}$$

In (Pagh, 2012), the compressed matrix multiplication is a sum of CS of outer products. Instead of using CS of each row/column of the input matrices to compute the approximated outer product, we use each row/column of the multi-dimensional tensor sketched matrices. Notice that since \mathcal{G} does not have any underlying structure, $MTS(\mathcal{G}) = MTS(vec(\mathcal{G})) = CS(vec(\mathcal{G}))$. The computation complexity of this estimation process is $O(nr + m_1 m_2 \log(m_1 m_2))$. The memory complexity is $O(m_1 m_2)$.

Suppose $\hat{\mathcal{T}}$ is the recovered tensor for $\mathcal{T} = \mathcal{G}(U, V, W)$ after applying MTS on U, V and W with sketching dimension

m_1 and m_2 along two modes and count sketch on \mathcal{G} with sketching dimension m_2 . Suppose the estimation takes d independent sketches of \mathcal{G} , U , V and W and then report the median of the d estimates:

Theorem 3.2 (MTS recovery analysis for Tucker tensor). If $d = \Omega(\log(1/\delta))$ and $m_1 m_2 = \Omega(\frac{r^3 \|G\|_F^2 \|U\|_F^2 \|V\|_F^2 \|W\|_F^2}{\epsilon^2})$, then with probability $\geq 1 - \delta$ there is $|\hat{\mathcal{T}}_{ijk} - T_{ijk}| \leq \epsilon$.

Theorem 3.2 shows that the product of sketch length $m_1 m_2$ can be set as $O(r^3)$ to provably approximate a 3rd-order Tucker-form tensor with dimension n , rank r . Given Theorem 3.1 and 3.2, if we set $c = O(r^3)$ and $m_1 m_2 = O(r^3)$, the estimation error for CTS and MTS will be at the same level. Detailed proofs for Theorem 3.1, Theorem 3.2 are in Appendix B.3.

REMARKS: CP-form Tensor Sketching CP-form tensor can be treated as a special case of Tucker-form tensor. For a third-order tensor: its core tensor is a sparse tensor: only diagonal data has non-zero values. We can write the decomposition as $\mathcal{T} = \sum_{i=1}^r \mathcal{G}_{iii} U_i \otimes V_i \otimes W_i$. We can sketch it in the same way as we described above. The only difference is that instead of sum over all \mathcal{G} values, we sum over only r number of \mathcal{G} values. We summarize the computation and memory analysis in Table 4 and 5. By performing MTS on the CP-form tensor components, we get a ratio of $O(r)$ improvement if the tensor is overcomplete ($r > n$).

3.1.3. COMPUTATION AND MEMORY ANALYSIS

The computation and memory cost is analyzed in Table 5. We get a computation cost improvement with a ratio of $O(r^2)$ if $r^3 < n$, $O(r^3)$ if $r^3 > n$, compared to previous CTS method for Tucker-form Tensor.

Table 4: Computation and memory analysis for Tucker/CP tensor sketching before substituting c, m_1, m_2 with known parameters.

Operator	Computation	Memory
Tucker		
CTS(\mathcal{T})	$O(nr^3 + cr^3 \log c)$	$O(cr + r^3)$
MTS(\mathcal{T})	$O(nr + r^3 + m_1 m_2 \log(m_1 m_2))$	$O(m_1 m_2)$
CP		
CTS(\mathcal{T})	$O(nr + cr \log c)$	$O(cr + r)$
MTS(\mathcal{T})	$O(nr + r + m_1 m_2 \log(m_1 m_2))$	$O(m_1 m_2)$

3.2. Tensor-Train Sketching: CTS vs. MTS

Tensor-train(TT) decomposition is another important tensor structure. For simplicity, we use a third-order tensor as an example. Assume $\mathcal{T} \in \mathbb{R}^{n_1 \times n_2 \times n_3}$, $G_1 \in \mathbb{R}^{n_1 \times r_1}$, $G_2 \in \mathbb{R}^{n_2 \times r_1 \times r_2}$, $G_3 \in \mathbb{R}^{n_3 \times r_2 \times 1}$, the TT format is: $\mathcal{T}_{i_1 i_2 i_3} = G_1[i_1, :, :] G_2[i_2, :, :] G_3[i_3, :, :]$, $\forall i_1 \in [n_1], i_2 \in [n_2], i_3 \in [n_3]$.

Table 5: Computation and memory analysis for Tucker/CP tensor sketching after substituting c, m_1, m_2 with known parameters (keep both methods with same recovery error).

Operator	Computation	Memory
Tucker		
\mathcal{T}	$O(n^3 r + n^2 r^2 + nr^3)$	$O(nr + r^3)$
CTS(\mathcal{T})	$O(nr^3 + r^6 \log r)$	$O(r^4)$
MTS(\mathcal{T})	$O(nr + r^3 \log r)$	$O(r^3)$
CP		
\mathcal{T}	$O(n^3 r^3)$	$O(nr + r)$
CTS(\mathcal{T})	$O(nr + r^2 \log r)$	$O(r^2)$
MTS(\mathcal{T})	$O(nr + r \log r)$	$O(r)$

[n_3]. By sketching G_1, G_2 and G_3 , we obtain an estimation of the TT format tensor. We assume $n_1 = n_2 = n_3 = n$, $r_1 = r_2 = r$.

- **CTS** Count sketch is done along the fibers of size n with sketching dimension c . In other word, $CS(G_1) \in \mathbb{R}^{c \times 1 \times r}$, $CS(G_2) \in \mathbb{R}^{c \times r \times r}$, $CS(G_3) \in \mathbb{R}^{c \times r \times 1}$. We can then use the method proposed by (Pagh, 2012) to compute a sequence of matrix multiplications.
- **MTS** We can rewrite the TT format as: $reshape(\mathcal{T}) = (G_1 \otimes G_3) reshape(G_2)$. $reshape(\mathcal{T}) \in \mathbb{R}^{n_1 n_3 \times n_2}$, $reshape(G_2) \in \mathbb{R}^{r^2 \times n_2}$. Algorithm 5 in Appendix A.2 shows the procedure steps.

Table 6: Computation and memory analysis for TT.

Operator	Computation	Memory
\mathcal{T}	$n^3 r^2$	$O(nr)$
CTS(\mathcal{T})	$O(nr^2 + cr^2 \log c + c)$	$O(nc)$
MTS(\mathcal{T})	$O(nr^2 + m_1 m_2 \log(m_1 m_2))$	$O(m_1 m_2)$

We put the error analysis for TT-form sketching in Appendix B.4. We show that if $c = O(r^2)$ and $m_1 m_2 = O(r^2)$, the recovery error will be the same for MTS and CTS methods. This gives us approximate $O(r^2)$ times improvement using MTS if $\log r > n$, comparing to the one using CS method.

4. Experiments

In this section, we present an empirical study of the multi-dimensional tensor sketch in matrix and tensor operations. The goals of this study are: a) establish that our method significantly compress the input without losing principle information from the data, b) demonstrate the advantages of MTS in compressing Kronecker product and tensor contraction operation in practice, compared to CTS, c) present potential application of MTS in deep learning tasks.

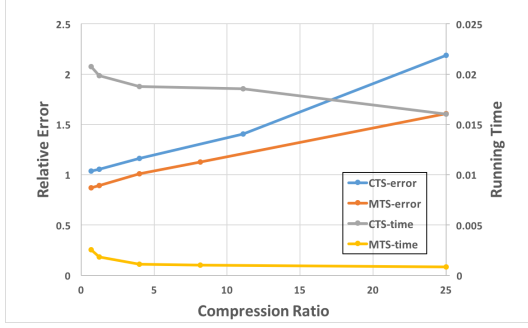


Figure 8: Kronecker product estimation for two 10×10 matrices.

4.1. Kronecker Product

We compress Kronecker products using CTS and MTS based on Figure 5 and Figure 6. We compute the recovery relative error and compression time verse the compression ratio. Given a Kronecker product matrix $C \in \mathbb{R}^{ab \times de}$, the $CTS(C) \in \mathbb{R}^{ab \times c}$, the $MTS(C) \in \mathbb{R}^{m_1 \times m_2}$. The compression ratio for CTS and MTS are $\frac{de}{c}$ and $\frac{abde}{m_1 m_2}$. The relative error is calculated as $\frac{\|C - \hat{C}\|_F}{\|C\|_F}$. The result is obtained by independently running the sketching 5 times and choosing the median. All inputs are randomly generated from the normal distribution.

From Figure 8, we show that the recovery error of CTS/MTS is proportional to the compression ratio, while the running time is inverse proportional to the compression ratio. MTS out performs CTS in aspect of relative error and running time when they keep the same compression ratio.

4.2. Covariance Matrix Estimation

Given a matrix $A \in \mathbb{R}^{10 \times 10}$, all entries are sampled independently and uniformly from $[-1, 1]$, except for rows two and nine which are positively correlated. In Figure 9, the upper middle figure is the true value of AA^T , the upper right figure is an approximation of AA^T using the algorithm in (Pagh, 2012) with a compression ratio of 2.5. Lower left is the true value of $A \otimes A^T$. By applying MS based on Figure 6 (Algorithm 4 in Appendix A.1), we get approximated $A \otimes A^T$ in the lower middle figure with a compression ratio of 6.25. Further, we estimate AA^T using the fact that $(AA^T)_{ij} = \sum_{k=1}^r (A \otimes A^T)_{r(i-1)+k, n(k-1)+j}$, if $A \in \mathbb{R}^{n \times r}$. In both methods, we repeat the sketching 300 times and use the median as the final estimation. The covariance matrix estimation quality using MTS is better than the one using CS, and it uses a higher compression rate.

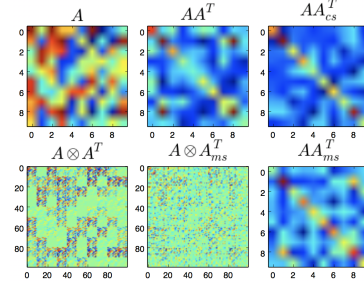


Figure 9: Covariance matrix estimation.

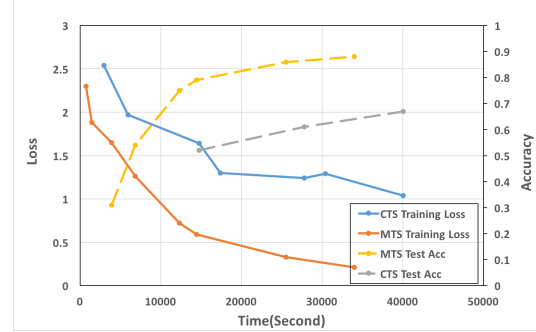


Figure 10: Training loss and test accuracy on CIFAR10 for different network structures.

4.3. Tensor Regression Network

To demonstrate the versatility of our method, we combine it with deep learning, by integrating it into a tensor regression network for object classification.

Kossaifi et al. (2017) propose the tensor regression layer (TRL) to express outputs through a low-rank multi-linear mapping. It learns a Tucker-form tensor weight for the high-order activation tensor. Instead of reconstructing the full regression weight tensor using tensor contractions, we propose to sketch it using Equation 7 and 8. In our experiments, we use a ResNet18 (He et al., 2016), from which the flattening and fully-connected layers are removed, and are replaced by our proposed sketched tensor regression layer. The network structure is illustrated in Figure 11.

We compare CTS and MTS on the CIFAR10 dataset (Krizhevsky, 2009). We report the learning loss and the test accuracy in Figure 10. Compared to CTS, MTS converges faster. In Figure 12, MTS-tensorized network still outperforms the non-tensorized network when the compression ratio is not too big. Compared to the original tensor regression network, we use 8 times fewer parameters with only 4% accuracy loss (original TRL has 25k parameters, sketched TRL has 3k). Final test accuracy using original TRL/sketched TRL is 95%/91%.

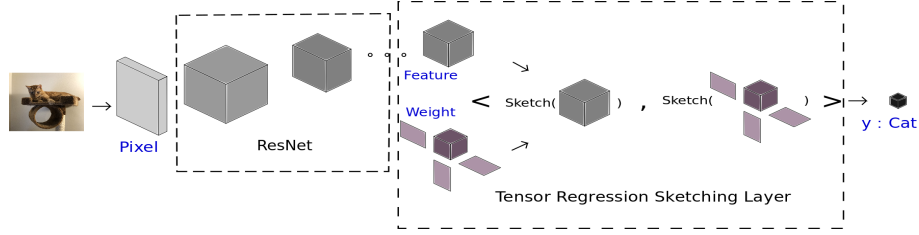


Figure 11: Tensor regression layer with sketching.

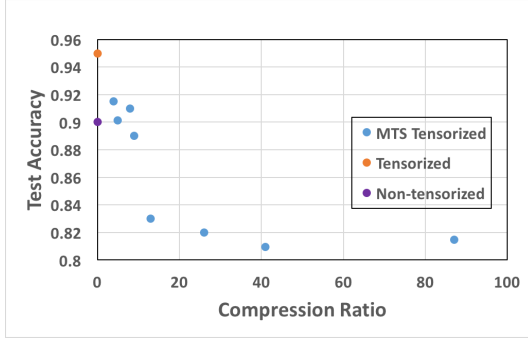


Figure 12: Test accuracy on CIFAR 10 for MTS tensorized network with different compression ratio(Compression ratio is respect to tensorized network. Compression ratio = 0 means no compression added).

5. Related Work

Given the importance of data approximation in the aspect of computation efficiency and privacy concerns, many methods have been developed to use fewer parameters in the estimation of the original data. As one might expect, data with a particular structure may require a specific approximation method. Truncated singular value decomposition (SVD) (Eckart & Young, 1936) is an approximation method to represent the rotation and rescale of the data. However, this decomposition may not fit for specific data that has sparsity/non-negativity constraints. CX and CUR matrix decompositions are proposed to solve this problem (Mahoney & Drineas, 2009; Caiafa & Cichocki, 2010).

Since structure in the data may not be respected by mathematical operations on the data, sketching is more interpretable and has better informing intuition (Bringmann & Panagiotou, 2017; Alon et al., 1999; Weinberger & Saul, 2009). Min-hash (Broder, 1997) is a technique for estimating how similar two sets of data are. An extension of that is one-bit CP-hash (Christiani et al., 2018). To make use of parallel computing resources, 2-of-3 cuckoo hashing (Amossen & Pagh, 2011) is proposed based on (Pagh & Rodler, 2001).

Count Sketch(CS) is first proposed by Charikar et al. (2002) to estimate the frequency of each element in a stream. Pagh (2012) propose a fast algorithm to compute count sketch

of an outer product of two vectors using FFT properties. They prove that the CS of the outer product is equal to the convolutions between the CS of each input. Tensor sketch is proposed by Pham & Pagh (2013) to approximate non-linear kernel. It can approximate any polynomial kernel in $O(N(n + c \log c))$ time, while previous methods require $O(Nnc)$ time for N training samples in n -dimensional space and c random feature maps. Wang et al. (2015) develop a novel approach for randomized computation of tensor contractions using tensor sketch, and apply it to fast tensor CP decomposition. However, all these sketching techniques are projecting tensors to vector space.

Besides above dimension reduction algorithms, efficient tensor contraction primitive is another focus in computation community. Jhurani & Mulleney (2015) propose low-overhead interface for multiple small matrix multiplications on NVIDIA GPUs. Shi et al. (2016) further present optimized computation primitives for single-index contractions involving all the possible configurations of second-order and third-order tensors.

6. Conclusion

In this paper, we propose a new sketching technique, called multi-dimensional tensor sketching (MTS). MTS is an unbiased estimator for tensors using sketching techniques along each mode. We present approximation algorithms for Kronecker product and tensor contraction. We improve both computational and memory requirement for tensor product and tensor contraction compared to previous sketching techniques, especially when tensors have high ranks. We apply the algorithms to synthetic and real data. In both cases, MTS performs efficient compression while preserving major information from the input.

References

- Alon, N., Matias, Y., and Szegedy, M. The space complexity of approximating the frequency moments. *Journal of Computer and System Sciences*, 58(1):137–147, February 1999.
- Amossen, R. R. and Pagh, R. A new data layout for set intersection on gpus. In *Proceedings of the 2011 IEEE International Parallel & Distributed Processing Symposium, IPDPS '11*, pp. 698–708, Washington, DC, USA, 2011. IEEE Computer Society. ISBN 978-0-7695-4385-7. doi: 10.1109/IPDPS.2011.71. URL <https://doi.org/10.1109/IPDPS.2011.71>.
- Anandkumar, A., Ge, R., Hsu, D., Kakade, S. M., and Telgarsky, M. Tensor decompositions for learning latent variable models. *The Journal of Machine Learning Research*, 15(1):2773–2832, 2014.
- Antol, S., Agrawal, A., Lu, J., Mitchell, M., Batra, D., Zitnick, C. L., and Parikh, D. VQA: Visual Question Answering. In *International Conference on Computer Vision (ICCV)*, 2015.
- Aza, Y., Fia, A., Karli, A. R., McSherr, F., and Sai, J. Spectral analysis of data. *STOC*, 2001.
- Bringmann, K. and Panagiotou, K. Efficient sampling methods for discrete distributions. *Algorithmica*, 79(2): 484–508, Oct 2017. ISSN 1432-0541. doi: 10.1007/s00453-016-0205-0. URL <https://doi.org/10.1007/s00453-016-0205-0>.
- Broder, A. Z. On the resemblance and containment of documents. *IEEE: Compression and Complexity of Sequences: Proceedings, Positano, Amalfitan Coast, Salerno, Italy*, 10:21–29, 1997.
- Caiafa, C. F. and Cichocki, A. Generalizing the column–row matrix decomposition to multi-way arrays. *Linear Algebra and its Applications*, 433:557–573, Sept 2010.
- Charikar, M., Chen, K., and Farach-Colton, M. Finding frequent items in data streams. In *Proceedings of ICALP'02*, pp. 693–703, 2002.
- Christiani, T., Pagh, R., and Sivertsen, J. Scalable and robust set similarity join. *The annual IEEE International Conference on Data Engineering*, 2018.
- Demaine, E. D., López-Ortiz, A., and Munro, J. I. Frequency estimation of internet packet streams with limited space. In *Proceedings of the 10th Annual European Symposium on Algorithms, ESA '02*, pp. 348–360, London, UK, UK, 2002. Springer-Verlag. ISBN 3-540-44180-8. URL <http://dl.acm.org/citation.cfm?id=647912.740658>.
- Eckart, C. and Young, G. The approximation of one matrix by another of lower rank. In *Psychometrika*. Springer-Verlag, 1936.
- Fukui, A., Park, D. H., Yang, D., Rohrbach, A., Darrell, T., and Rohrbach, M. Multimodal compact bilinear pooling for visual question answering and visual grounding. *EMNLP 2016*, 2016.
- Harshman, R. Foundations of the parafac procedure: Models and conditions for an explanatory multi-model factor analysis. *UCLA Working Papers in Phonetics*, 16: 1–84, 1970. URL <http://citeseerx.ist.psu.edu/viewdoc/download?doi=10.1.1.144.5652&rep=rep1&type=pdf>.
- He, K., Zhang, X., Ren, S., and Sun, J. Deep residual learning for image recognition. In *Proceedings of the IEEE Conference on Computer Vision and Pattern Recognition (CVPR)*, 2016.
- Jhurani, C. and Mulleney, P. A gemm interface and implementation on nvidia gpus for multiple small matrices. *J. of Parallel and Distributed Computing*, pp. 133–140, 2015.
- Koren, Y., Bell, R., and Volinsky, C. Matrix factorization techniques for recommender systems. *IEEE Computer Society*, 2009.
- Kossaifi, J., Lipton, Z. C., Khanna, A., Furlanello, T., and Anandkumar, A. Tensor regression networks. 2017. URL <http://arxiv.org/abs/1707.08308>.
- Krizhevsky, A. Learning multiple layers of features from tiny images. Technical report, 2009.
- Mahoney, M. W. and Drineas, P. Cur matrix decompositions for improved data analysis. *Proceedings of the National Academy of Sciences*, 106(3):697–702, 2009. ISSN 0027-8424. doi: 10.1073/pnas.0803205106.
- Oseledets, I. V. Tensor-train decomposition. *SIAM J. Sci. Comput*, 33(5):2295–2317, 2011.
- Pagh, R. Compressed matrix multiplication. *ITCS*, 2012.
- Pagh, R. and Rodler, F. F. Cuckoo hashing. *Lecture Notes in Computer Science*, 2001. doi: 10.1007/3-540-44676-1_10.
- Pham, N. and Pagh, R. Fast and scalable polynomial kernels via explicit feature maps. *KDD*, 2013.
- Shi, Y., Niranjan, U., Anandkumar, A., and Cecka, C. Tensor contractions with extended blas kernels on cpu and gpu. *HiPC*, 2016.

- Shi, Y., Furlanello, T., Zha, S., and Anandkumar, A. Question type guided attention in visual question answering. *ECCV*, 2018.
- Springer, P., Su, T., and Bientinesi, P. Hptt: A high-performance tensor transposition c++ library. *Proceedings of the 4th ACM SIGPLAN International Workshop on Libraries, Languages, and Compilers for Array Programming*, 2017.
- Teney, D., Anderson, P., He, X., and van den Hengel, A. Tips and tricks for visual question answering: Learnings from the 2017 challenge,. *CVPR 2017 VQA Workshop*, 2017. URL <http://arxiv.org/abs/1708.02711>.
- Tucker, L. R. Some mathematical notes on three-mode factor analysis. *Psychometrika*, 31(3):279–311, 1966. doi: 10.1007/BF02289464.
- Wang, Y., Tung, H.-Y., Smola, A., and Anandkumar, A. Fast and guaranteed tensor decomposition via sketching. *Proceedings of Advances in Neural Information Processing Systems (NIPS)*, 2015.
- Weinberger, K. Q. and Saul, L. K. Distance metric learning for large margin nearest neighbor classification. *Journal of Machine Learning Research*, 10:207–244, 2009.
- Yu, R., Zheng, S., Anandkumar, A., and Yue, Y. Long-term forecasting using tensor-train rnns.

A. List of some algorithms mentioned in the main paper

A.1. Kronecker Product Sketching

Algorithm 4 Compress/Decompress Kronecker Product

```

1: procedure COMPRESS-KP( $A, B, m_1, m_2$ )  $\triangleright A \in \mathbb{R}^{n_1 \times n_2}, B \in \mathbb{R}^{n_3 \times n_4}$ 
2:   for  $X$  in  $[A, B]$  do
3:      $X^{ms} = \text{MTS}(X, [m_1, m_2])$ 
4:    $\text{FFT2}(A^{ms}), \text{FFT2}(B^{ms})$ 
5:    $P = \text{IFFT2}(A^{ms} \circ B^{ms})$ 
6:   return ( $P$ )
7:
8: procedure DECOMPRESS-KP( $P$ )
9:    $C = \text{zeros}(n_1 n_3, n_2 n_4)$ 
10:  for  $w, q, o, g := 1$  to  $n_1, n_2, n_3, n_4$  do
11:     $k = (h_{A1}[w] + h_{B1}[o]) \bmod m_1$ 
12:     $l = (h_{A2}[q] + h_{B2}[g]) \bmod m_2$ 
13:     $\text{tmp} = s_{A1}[w] s_{A2}[q] s_{B1}[o] s_{B2}[g] P[k, l]$ 
14:     $i = n_3(w - 1) + o$ 
15:     $j = n_4(q - 1) + g$ 
16:     $C_{ij} = \text{tmp}$ 
17:  return ( $C$ )

```

A.2. Tensor-Train Sketching

Algorithm 5 TT Sketching: $\text{MTS}(T) = \text{MTS}(G_1 G_2 G_3)$

```

procedure COMPRESS( $G_1, G_2, G_3, m_1, m_2, d$ )  $\triangleright G_1 \in \mathbb{R}^{n_1 \times r_1}, G_2 \in \mathbb{R}^{n_2 \times r_1 \times r_2}, G_3 \in \mathbb{R}^{n_3 \times r_2}$ 
  for  $X$  in  $[G_1, G_3]$  do
     $X^{ms} = \text{MTS}(X, [m_1, m_2])$ 
   $\text{reshape}(G_2) \in \mathbb{R}^{r_1 r_2 \times n_2}$ 
   $G_2^{ms} = \text{MTS}(G_2, [m_2, m_1])$ 
   $\text{FFT2}(G_1^{ms}), \text{FFT2}(G_2^{ms}), \text{FFT2}(G_3^{ms})$ 
   $Q = G_1^{ms} \circ G_3^{ms}$ 
  for  $k := 1$  to  $m_2$  do
     $P += Q[:, k] \circ G_2^{ms}[k, :]$ 
  return ( $\text{IFFT2}(P)$ )

procedure DECOMPRESS( $P$ )
   $C = \text{zeros}(n_1 n_2 n_3)$ 
  for  $w, g, o := 1$  to  $n_1, n_2, n_3$  do
     $k = (h_{G1}[w] + h_{G22}[g] + h_{G31}[o]) \bmod m_1$ 
     $\text{tmp} = s_{G11}[w] s_{G22}[g] s_{G31}[o] P[k]$ 
     $C_{wgo} = \text{tmp}$ 
  return ( $C$ )

```

B. Proofs of some technical theorems/lemmas

B.1. MS of the Kronecker product

Lemma B.1. Given two matrices $A \in \mathbb{R}^{n \times n}, B \in \mathbb{R}^{n \times n}$,

$$\begin{aligned}
 \text{MTS}(A \otimes B) &= \text{MTS}(A) * \text{MTS}(B) \\
 &= \text{IFFT2}(\text{FFT2}(\text{MTS}(A)) \circ \text{FFT2}(\text{MTS}(B)))
 \end{aligned} \tag{9}$$

Proof of Lemma B.1. The Kronecker product defines $(A \otimes B)_{n_3(p-1)+h, n_4(q-1)+g} = A_{pq}B_{hg}$. Thus:

$$\begin{aligned}
 & \sum_{pqhg} (A \otimes B)_{ab} s_1(p) s_2(q) s_3(h) s_4(g) w^{t_1 h_a + t_2 h_b} \\
 &= \sum_{pqhg} A_{pq} B_{hg} s_1(p) s_2(q) s_3(h) s_4(g) w^{t_1 h_a + t_2 h_b} \\
 &= \sum_{pq} A_{pq} s_1(p) s_2(q) w^{t_1 h_1(p) + t_2 h_2(q)} \sum_{hg} B_{hg} s_3(h) s_4(g) w^{t_1 h_3(h) + t_2 h_4(g)} \\
 &= FFT2(MTS(A)) \circ FFT2(MTS(B))
 \end{aligned} \tag{10}$$

where $a = n_3(p-1) + h$, $b = n_4(q-1) + g$, $h_a = h_1(p) + h_3(h)$, $h_b = h_2(q) + h_4(g)$.

Assign $i = n_3(p-1) + h$, $j = n_4(q-1) + g$, $s_5(i) = s_1(p)s_3(h)$, $s_6(j) = s_2(q)s_4(g)$, $h_5(i) = h_1(p) + h_3(h)$ and $h_6(j) = h_2(q) + h_4(g)$, we have

$$\begin{aligned}
 & \sum_{pqhg} (A \otimes B)_{ab} s_1(p) s_2(q) s_3(h) s_4(g) w^{t_1 h_a + t_2 h_b} \\
 &= \sum_{ij} (A \otimes B)_{ij} s_5(i) s_6(j) w^{t_1 h_5(i) + t_2 h_6(j)} \\
 &= FFT2(MTS(A \otimes B)) \\
 &= FFT2(MTS(A)) \circ FFT2(MS(B))
 \end{aligned} \tag{11}$$

Consequently, we have $MTS(A \otimes B) = IFFT2(FFT2(MTS(A)) \circ FFT2(MTS(B)))$. The recovery map is $A \hat{\otimes} B_{n_3(p-1)+h, n_4(q-1)+g} = s_1(p)s_2(q)s_3(h)s_4(g)MTS(A \otimes B)_{(h_1(p)+h_3(h)) \bmod m_1, (h_2(q)+h_4(g)) \bmod m_2}$ for $p \in [n_1]$, $q \in [n_2]$, $h \in [n_3]$, $g \in [n_4]$. \square

B.2. Analysis of CS and MTS approximation error

Theorem B.2 ((Charikar et al., 2002)). Given a vector $u \in \mathbb{R}^n$, **CS** hashing functions s and h with sketching dimension c , for any i^* , the recovery function $\hat{u}(i^*) = s(i^*)CS(u)(h(i^*))$ computes an unbiased estimator for $u(i^*)$ with variance bounded by $\|u\|_2^2/c$.

Proof of Theorem B.2. For $i \in \{1, 2, \dots, n\}$, let K_i be the indicator variable for the event $h(i) = h(i^*)$. We can write $\hat{u}(i^*)$ as

$$\hat{u}(i^*) = s(i^*) \sum_i K_i s(i) u(i) \tag{12}$$

Observe that $K_i = 1$, if $i = i^*$, $\mathbf{E}(s(i^*)s(i)) = 0$, for all $i \neq i^*$, and $\mathbf{E}(s(i^*)^2) = 1$, we have

$$\begin{aligned}
 \mathbf{E}(\hat{u}(i^*)) &= \mathbf{E}(s(i^*)K_{i^*}s(i^*)u(i^*)) + \mathbf{E}(s(i^*) \sum_{i \neq i^*} K_i s(i) u(i)) \\
 &= u(i^*)
 \end{aligned} \tag{13}$$

To bound the variance, we rewrite the recovery function as

$$\hat{u}(i^*) = s(i^*)K_{i^*}s(i^*)u(i^*) + s(i^*) \sum_{i \neq i^*} K_i s(i) u(i) \tag{14}$$

To simplify notation, we assign X as the first term, Y as the second term. $\mathbf{Var}(X) = 0$, and $COV(X, Y) = 0$ since $s(i)$ for $i \in \{1, 2, \dots, n\}$ are 2-wise independent. Thus,

$$\mathbf{Var}(X + Y) = \sum_{i \neq i^*} Var(K_i s(i^*) s(i) u(i)) \tag{15}$$

$\mathbf{E}(K_i s(i^*) s(i) u(i)) = 0$ for $i \neq i^*$. Consequently,

$$\mathbf{Var}(K_i s(i^*) s(i) u(i)) = \mathbf{E}((K_i s(i^*) s(i) u(i))^2) = \mathbf{E}(K_i^2) u(i)^2 = u(i)^2 / c \quad (16)$$

The last equality uses that $\mathbf{E}(K_i^2) = \mathbf{E}(K_i) = 1/c$, for all $i \neq i^*$. Summing over all terms, we have $\mathbf{Var}(\hat{u}(i^*)) \leq \|u\|_2^2 / c$. \square

Proof of Theorem 2.1. For $i \in \{1, 2, \dots, n_1\}$, $j \in \{1, 2, \dots, n_2\}$, let K_{ij} be the indicator variable for the event $h_1(i) = h_1(i^*)$ and $h_2(j) = h_2(j^*)$. We can write $\hat{U}_{i^*j^*}$ as

$$\hat{U}_{i^*j^*} = s_1(i^*) s_2(j^*) \sum_{ij} K_{ij} s_1(i) s_2(j) U_{ij} \quad (17)$$

Observe that $K_{ij} = 1$, if $i = i^*$, $j = j^*$. $\mathbf{E}(s_1(i^*) s_1(i)) = 0$, $\mathbf{E}(s_2(j^*) s_2(j)) = 0$, for all $i \neq i^*$, $j \neq j^*$, and $\mathbf{E}(s_1(i^*)^2) = 1$, $\mathbf{E}(s_2(j^*)^2) = 1$, we have

$$\begin{aligned} \mathbf{E}(\hat{U}_{i^*j^*}) &= \mathbf{E}(s_1^2(i^*) s_2^2(j^*) K_{i^*j^*} U_{i^*j^*}) + \mathbf{E}(s_1(i^*) s_2(j^*) \sum_{i \neq i^*, j \neq j^*} K_{ij} s_1(i) s_2(j) U_{ij}) \\ &= U_{i^*j^*} \end{aligned} \quad (18)$$

To bound the variance, we rewrite the recovery function as

$$\hat{U}_{i^*j^*} = s_1^2(i^*) s_2^2(j^*) K_{i^*j^*} U_{i^*j^*} + s_1(i^*) s_2(j^*) \sum_{i \neq i^*, j \neq j^*} K_{ij} s_1(i) s_2(j) U_{ij} \quad (19)$$

To simplify notation, we assign X as the first term, Y as the second term. $\mathbf{Var}(X) = 0$, and $\text{COV}(X, Y) = 0$ since $s_1(i)$ and $s_2(j)$ for $i \in \{1, 2, \dots, n_1\}$, $j \in \{1, 2, \dots, n_2\}$ are both 2-wise independent. Thus,

$$\mathbf{Var}(X + Y) = \sum_{i \neq i^*, j \neq j^*} \mathbf{Var}(K_{ij} s_1(i^*) s_2(j^*) s_1(i) s_2(j) U_{ij}) \quad (20)$$

$\mathbf{E}(K_{ij} s_1(i^*) s_2(j^*) s_1(i) s_2(j) U_{ij}) = 0$ for $i \neq i^*$, $j \neq j^*$. Consequently,

$$\mathbf{Var}(K_{ij} s_1(i^*) s_2(j^*) s_1(i) s_2(j) U_{ij}) = \mathbf{E}((K_{ij} s_1(i^*) s_2(j^*) s_1(i) s_2(j) U_{ij})^2) = \mathbf{E}(K_{ij}^2) U_{ij}^2 = U_{ij}^2 / (m_1 m_2) \quad (21)$$

The last equality uses that $\mathbf{E}(K_{ij}^2) = \mathbf{E}(K_{ij}) = 1/(m_1 m_2)$, for all $i \neq i^*$, $j \neq j^*$. Summing over all terms, we have $\mathbf{Var}(\hat{U}_{i^*j^*}) \leq \|U\|_F^2 / (m_1 m_2)$. \square

B.3. Analysis of Tucker-form tensor approximation error

Proof of Theorem 3.1. We first prove the unbiasedness.

$$\begin{aligned} \mathbf{E}(\hat{\mathcal{T}}_{ijk}) &= \sum_{a=1}^r \sum_{b=1}^r \sum_{c=1}^r \mathcal{G}_{abc} \mathbf{E}(\hat{U}_{ia} \hat{V}_{jb} \hat{W}_{kc}) \\ &= \sum_{a=1}^r \sum_{b=1}^r \sum_{c=1}^r \mathcal{G}_{abc} \mathbf{E}(\hat{U}_{ia}) \mathbf{E}(\hat{V}_{jb}) \mathbf{E}(\hat{W}_{kc}) \\ &= \sum_{a=1}^r \sum_{b=1}^r \sum_{c=1}^r \mathcal{G}_{abc} U_{ia} V_{jb} W_{kc} \\ &= \mathcal{T}_{ijk} \end{aligned} \quad (22)$$

The second step uses the property that the elements are independent. The third step is obtained using Theorem B.2.

$$\begin{aligned}
 \mathbf{Var}(\hat{\mathcal{T}}_{ijk}) &= \sum_{a=1}^r \sum_{b=1}^r \sum_{c=1}^r \mathcal{G}_{abc} \mathbf{Var}(\hat{U}_{ia} \hat{V}_{jb} \hat{W}_{kc}) \\
 &= \sum_{a=1}^r \sum_{b=1}^r \sum_{c=1}^r \mathcal{G}_{abc} (\mathbf{Var}(\hat{U}_{ia}) \mathbf{Var}(\hat{V}_{jb}) \mathbf{Var}(\hat{W}_{kc}) + \mathbf{E}^2(\hat{U}_{ia}) \mathbf{Var}(\hat{V}_{jb}) \mathbf{Var}(\hat{W}_{kc}) \\
 &\quad + \mathbf{E}^2(\hat{V}_{jb}) \mathbf{Var}(\hat{U}_{ia}) \mathbf{Var}(\hat{W}_{kc}) + \mathbf{E}^2(\hat{W}_{kc}) \mathbf{Var}(\hat{U}_{ia}) \mathbf{Var}(\hat{V}_{jb}) \\
 &\quad + \mathbf{E}^2(\hat{U}_{ia}) \mathbf{E}^2(\hat{V}_{jb}) \mathbf{Var}(\hat{W}_{kc}) + \mathbf{E}^2(\hat{V}_{jb}) \mathbf{E}^2(\hat{W}_{kc}) \mathbf{Var}(\hat{U}_{ia}) \\
 &\quad + \mathbf{E}^2(\hat{U}_{ia}) \mathbf{E}^2(\hat{W}_{kc}) \mathbf{Var}(\hat{V}_{jb})) \\
 &\leq \sum_{a=1}^r \sum_{b=1}^r \sum_{c=1}^r \mathcal{G}_{abc} \left(\frac{\|U_a\|_2^2 \|V_b\|_2^2 \|W_c\|_2^2}{c^3} + \frac{U_{ia}^2 \|V_b\|_2^2 \|W_c\|_2^2}{c^2} \right. \\
 &\quad \left. + \frac{V_{jb}^2 \|U_a\|_2^2 \|W_c\|_2^2}{c^2} + \frac{W_{kc}^2 \|U_a\|_2^2 \|V_b\|_2^2}{c^2} + \frac{U_{ia}^2 V_{jb}^2 \|W_c\|_2^2}{c} + \frac{V_{jb}^2 W_{kc}^2 \|U_a\|_2^2}{c} + \frac{U_{ia}^2 W_{kc}^2 \|V_b\|_2^2}{c} \right) \\
 &\leq r^3 g \|U_a\|_2^2 \|V_b\|_2^2 \|W_c\|_2^2 \left(\frac{1}{c^3} + \frac{3}{c^2} + \frac{3}{c} \right) \\
 &\leq 7r^3 g \|U_a\|_2^2 \|V_b\|_2^2 \|W_c\|_2^2 \frac{1}{c}
 \end{aligned} \tag{23}$$

□

Computation complexity analysis CTS(\mathcal{T}) can be computed using $O(r^3(n + c \log c + c))$ operators: Inside r^3 summations, it takes $O(n)$ to do the count sketch for each column of U, V , and W , $O(c \log c)$ to do FFT/IFFT, and $O(c)$ to do element-wise product between the FFT results. The memory complexity is $O(cr + r^3)$: $O(cr)$ to store the count sketch results of U, V, W , $O(r^3)$ to store \mathcal{G} .

Proof of Theorem 3.2.

$$\begin{aligned}
 \mathbf{E}(\hat{\mathcal{T}}_{ijk}) &= \mathbf{E} \left(\sum_{l=1}^{r^3} (\hat{U} \otimes \hat{V} \otimes \hat{W})_{ijk} \text{vec}(\hat{\mathcal{G}})_l \right) \\
 &= \sum_{l=1}^{r^3} \mathbf{E}(\hat{U} \otimes \hat{V} \otimes \hat{W})_{ijk} \mathbf{E}(\text{vec}(\hat{\mathcal{G}})_l) \\
 &= \sum_{l=1}^{r^3} (U \otimes V \otimes W)_{ijk} \text{vec}(\mathcal{G})_l \\
 &= \mathcal{T}_{ijk}
 \end{aligned} \tag{24}$$

This is an unbiased estimator because both MS and CS are unbiased. For the variance, we have:

$$\begin{aligned}
 \mathbf{Var}(\hat{\mathcal{T}}_{ijk}) &= \mathbf{Var} \left(\sum_{l=1}^{r^3} (\hat{U} \otimes \hat{V} \otimes \hat{W})_{ijk} \text{vec}(\hat{\mathcal{G}})_l \right) \\
 &= \sum_{l=1}^{r^3} \mathbf{Var}(\hat{U} \otimes \hat{V} \otimes \hat{W})_{ijk} \text{vec}(\hat{\mathcal{G}})_l
 \end{aligned} \tag{25}$$

To simplify the notation, we set $X = \hat{U} \otimes \hat{V} \otimes \hat{W}$, $Y = \text{vec}(\hat{\mathcal{G}})$.

From kronecker product definition, we know $\exists a, b, c, d, e, f, X_{tl} = \hat{U}_{ab} \hat{V}_{cd} \hat{W}_{ef}$, for $\forall t, l$. Thus, $\mathbf{Var}(X_{tl}) =$

$$\mathbf{Var}(\hat{U}_{ab}\hat{V}_{cd}\hat{W}_{ef}).$$

$$\begin{aligned}
 \mathbf{Var}(\hat{U}_{ab}\hat{V}_{cd}\hat{W}_{ef}) &= \mathbf{Var}(\hat{U}_{ab})\mathbf{Var}(\hat{V}_{cd})\mathbf{Var}(\hat{W}_{ef}) + \mathbf{E}^2(\hat{U}_{ab})\mathbf{Var}(\hat{V}_{cd})\mathbf{Var}(\hat{W}_{ef}) \\
 &\quad + \mathbf{E}^2(\hat{V}_{cd})\mathbf{Var}(\hat{U}_{ab})\mathbf{Var}(\hat{W}_{ef}) + \mathbf{E}^2(\hat{W}_{ef})\mathbf{Var}(\hat{U}_{ab})\mathbf{Var}(\hat{V}_{cd}) \\
 &\quad + \mathbf{E}^2(\hat{U}_{ab})\mathbf{E}^2(\hat{V}_{cd})\mathbf{Var}(\hat{W}_{ef}) + \mathbf{E}^2(\hat{V}_{cd})\mathbf{E}^2(\hat{W}_{ef})\mathbf{Var}(\hat{U}_{ab}) \\
 &\quad + \mathbf{E}^2(\hat{U}_{ab})\mathbf{E}^2(\hat{W}_{ef})\mathbf{Var}(\hat{V}_{cd}) \\
 &= \frac{\|U\|_F^2\|V\|_F^2\|W\|_F^2}{(m_1m_2)^3} + \frac{U_{ab}^2\|V\|_F^2\|W\|_F^2}{(m_1m_2)^2} \\
 &\quad + \frac{V_{cd}^2\|U\|_F^2\|W\|_F^2}{(m_1m_2)^2} + \frac{W_{ef}^2\|U\|_F^2\|V\|_F^2}{(m_1m_2)^2} \\
 &\quad + \frac{U_{ab}^2V_{cd}^2\|W\|_F^2}{m_1m_2} + \frac{V_{cd}^2W_{ef}^2\|U\|_F^2}{m_1m_2} + \frac{U_{ab}^2W_{ef}^2\|V\|_F^2}{m_1m_2} \\
 &\leq 7\|U\|_F^2\|V\|_F^2\|W\|_F^2 \frac{1}{m_1m_2}
 \end{aligned} \tag{26}$$

We know $\mathbf{Var}(Y_l) = \frac{\|\mathcal{G}\|_F^2}{m_2}$, $\mathbf{E}(X_{tl}) = U_{ab}V_{cd}W_{ef}$, $\mathbf{E}(Y_l) = \mathcal{G}_l$. Thus,

$$\begin{aligned}
 \mathbf{Var}(\mathcal{T}_{ijk}) &= \mathbf{Var}\left(\sum_l^{r^3} X_{tl} Y_l\right) \\
 &= \sum_l^{r^3} \mathbf{Var}(X_{tl})\mathbf{Var}(Y_l) + \mathbf{E}^2(X_{tl})\mathbf{Var}(Y_l) + \mathbf{E}^2(Y_l)\mathbf{Var}(X_{tl}) \\
 &\leq \sum_l^{r^3} 7\|U\|_F^2\|V\|_F^2\|W\|_F^2\|\mathcal{G}\|_F^2 \frac{1}{m_1m_2^2} + \mathbf{E}^2(X_{tl})\frac{\|\mathcal{G}\|_F^2}{m_2} + \mathbf{E}^2(Y_l)7\|U\|_F^2\|V\|_F^2\|W\|_F^2 \frac{1}{m_1m_2} \\
 &\leq \sum_l^{r^3} \|U\|_F^2\|V\|_F^2\|W\|_F^2\|\mathcal{G}\|_F^2 \left(\frac{7}{m_1m_2^2} + \frac{1}{m_2} + \frac{7}{m_1m_2}\right) \\
 &\leq c_0 r^3 \|U\|_F^2\|V\|_F^2\|W\|_F^2\|\mathcal{G}\|_F^2 \frac{1}{m_1m_2}
 \end{aligned} \tag{27}$$

c_0 is a constant number such that $c_0 \geq 7 + m_1 + \frac{7}{m_2}$.

From Chebychev's inequality, if we run this sketch d times, where $d = \Omega(\log(1/\delta))$, we can get the desired error bond with probability at least $1 - \delta$.

Computation complexity analysis Overall, this sketch requires $O(nr + r^3 + m_1m_2 \log(m_1m_2) + m_1m_2)$ operations if m_1, m_2 are the sketching lengths for the two modes for U, V, W : it takes $O(nr + r^3)$ to do the MTS for U, V, W and CS for $\text{vec}(\mathcal{G})$. FFT2 requires $O(m_1m_2 \log(m_1m_2))$. We also need m_1m_2 operations to complete the element-wise product computation. The memory complexity is $O(m_1m_2)$. \square

B.4. Analysis of Tensor-Train form tensor approximation error

Theorem B.3. Suppose $\hat{\mathcal{T}} \in \mathbb{R}^{n \times n \times n}$ where $\hat{\mathcal{T}} = \hat{G}_1\hat{G}_2\hat{G}_3$, $\hat{G}_1 \in \mathbb{R}^{n \times r}$, $\hat{G}_2 \in \mathbb{R}^{n \times r \times r}$, $\hat{G}_3 \in \mathbb{R}^{n \times r}$. $\hat{\mathcal{T}}$ is the recovered tensor for $\mathcal{T} = G_1G_2G_3$ after applying count sketch on G_1, G_2 and G_3 with sketching dimension c . Suppose the estimation takes d independent sketches of G_1, G_2 and G_3 and then report the median of the d estimates. If $d = \Omega(\log(nr^2/\delta))$, $\max(\|G_1[:, l_1]\|_2) = g_1$, $\max(\|G_2[:, l_1, l_2]\|_2) = g_2$, $\max(\|G_3[:, l_2]\|_2) = g_3$ where $l_1 \in [r]$, $l_2 \in [r]$, and $c = \Omega(\frac{7r^2g_1^2g_2^2g_3^2}{\epsilon^2})$, then with probability $\geq 1 - \delta$ there is $|\hat{\mathcal{T}}_{ijk} - \mathcal{T}_{ijk}| \leq \epsilon$.

Proof of Theorem B.3.

$$\begin{aligned}
 \mathbf{Var}(\hat{T}_{ijk}) &= \mathbf{Var}(\hat{G}_1[i]\hat{G}_2[j]\hat{G}_3[k]) \\
 &= \mathbf{Var}\left(\sum_{l_1=1}^r \sum_{l_2=1}^r G_1[i, l_1]G_2[j, l_1, l_2]G_3[k, l_2]\right) \\
 &= \sum_{l_1=1}^r \sum_{l_2=1}^r \mathbf{Var}(\hat{G}_1[i, l_1])\mathbf{Var}(\hat{G}_2[j, l_1, l_2])\mathbf{Var}(\hat{G}_3[k, l_2]) + \mathbf{E}^2(\hat{G}_1[i, l_1])\mathbf{Var}(\hat{G}_2[j, l_1, l_2])\mathbf{Var}(\hat{G}_3[k, l_2]) \\
 &\quad + \mathbf{E}^2(\hat{G}_2[j, l_1, l_2])\mathbf{Var}(\hat{G}_1[i, l_1])\mathbf{Var}(\hat{G}_3[k, l_2]) + \mathbf{E}^2(\hat{G}_3[k, l_2])\mathbf{Var}(\hat{G}_1[i, l_1])\mathbf{Var}(\hat{G}_2[j, l_1, l_2]) \\
 &\quad + \mathbf{E}^2(\hat{G}_1[i, l_1])\mathbf{E}^2(\hat{G}_2[j, l_1, l_2])\mathbf{Var}(\hat{G}_3[k, l_2]) + \mathbf{E}^2(\hat{G}_2[j, l_1, l_2])\mathbf{E}^2(\hat{G}_3[k, l_2])\mathbf{Var}(\hat{G}_1[i, l_1]) \\
 &\quad + \mathbf{E}^2(\hat{G}_1[i, l_1])\mathbf{E}^2(\hat{G}_3[k, l_2])\mathbf{Var}(\hat{G}_2[j, l_1, l_2]) \\
 &\leq \sum_{l_1=1}^r \sum_{l_2=1}^r \frac{\|G_1[:, l_1]\|_2^2 \|G_2[:, l_1, l_2]\|_2^2 \|G_3[:, l_2]\|_2^2}{c^3} + \frac{G_1^2[i, l_1] \|G_2[:, l_1, l_2]\|_2^2 \|G_3[:, l_2]\|_2^2}{c^2} \\
 &\quad + \frac{G_2^2[j, l_1, l_2] \|G_1[:, l_1]\|_2^2 \|G_3[:, l_2]\|_2^2}{c^2} + \frac{G_3^2[k, l_2] \|G_2[:, l_1, l_2]\|_2^2 \|G_1[:, l_1]\|_2^2}{c^2} \\
 &\quad + \frac{G_1^2[i, l_1] G_2^2[j, l_1, l_2] \|G_3[:, l_2]\|_2^2}{c} + \frac{G_2^2[j, l_1, l_2] G_3^2[k, l_2] \|G_1[:, l_1]\|_2^2}{c} + \frac{G_1^2[i, l_1] G_3^2[k, l_2] \|G_2[:, l_1, l_2]\|_2^2}{c} \\
 &\leq r^2 G_{1a}^2 G_{2b}^2 G_{3c}^2 \left(\frac{1}{c^3} + \frac{3}{c^2} + \frac{3}{c} \right) \\
 &\leq 7r^2 G_{1a}^2 G_{2b}^2 G_{3c}^2 \frac{1}{c}
 \end{aligned} \tag{28}$$

when we assume $G_{1a} = \max(G_1[:, l_1])$, $G_{2b} = \max(G_2[:, l_1, l_2])$, $G_{3c} = \max(G_3[:, l_2])$ for $l_1 \in [r_1]$, $l_2 \in [r_2]$. \square

Theorem B.4. Suppose $\hat{\mathcal{T}} \in \mathbb{R}^{n \times n \times n}$ where $\hat{\mathcal{T}} = \hat{G}_1 \hat{G}_2 \hat{G}_3$, $\hat{G}_1 \in \mathbb{R}^{n \times r}$, $\hat{G}_2 \in \mathbb{R}^{n \times r \times r}$, $\hat{G}_3 \in \mathbb{R}^{n \times r}$. $\hat{\mathcal{T}}$ is the recovered tensor for $\mathcal{T} = G_1 G_2 G_3$ after applying multi-dimensional tensor sketch on G_1 , *reshape*(G_2) and G_3 with sketching dimension m_1 , m_2 . Suppose the estimation takes d independent sketches of G_1 , *reshape*(G_2) and G_3 and then report the median of the d estimates. If $d = \Omega(\log(nr^2/\delta))$, $\max(\|G_1\|_F) = g_1$, $\max(\|G_2\|_F) = g_2$, $\max(\|G_3\|_F) = g_3$ and $m_1 m_2 = \Omega(\frac{7r^2 g_1^2 g_2^2 g_3^2}{\epsilon^2})$, then with probability $\geq 1 - \delta$ there is $|\hat{\mathcal{T}}_{ijk} - T_{ijk}| \leq \epsilon$.

Proof of Theorem B.4.

$$\begin{aligned}
 \mathbf{Var}(\hat{T}_{ijk}) &= \mathbf{Var}(\hat{G}_1[i]\hat{G}_2[j]\hat{G}_3[k]) \\
 &= \mathbf{Var}\left(\sum_{l_1=1}^r \sum_{l_2=1}^r G_1[i, l_1]G_2[j, l_1, l_2]G_3[k, l_2]\right) \\
 &= \sum_{l_1=1}^r \sum_{l_2=1}^r \mathbf{Var}(\hat{G}_1[i, l_1])\mathbf{Var}(\hat{G}_2[j, l_1, l_2])\mathbf{Var}(\hat{G}_3[k, l_2]) + \mathbf{E}^2(\hat{G}_1[i, l_1])\mathbf{Var}(\hat{G}_2[j, l_1, l_2])\mathbf{Var}(\hat{G}_3[k, l_2]) \\
 &\quad + \mathbf{E}^2(\hat{G}_2[j, l_1, l_2])\mathbf{Var}(\hat{G}_1[i, l_1])\mathbf{Var}(\hat{G}_3[k, l_2]) + \mathbf{E}^2(\hat{G}_3[k, l_2])\mathbf{Var}(\hat{G}_1[i, l_1])\mathbf{Var}(\hat{G}_2[j, l_1, l_2]) \\
 &\quad + \mathbf{E}^2(\hat{G}_1[i, l_1])\mathbf{E}^2(\hat{G}_2[j, l_1, l_2])\mathbf{Var}(\hat{G}_3[k, l_2]) + \mathbf{E}^2(\hat{G}_2[j, l_1, l_2])\mathbf{E}^2(\hat{G}_3[k, l_2])\mathbf{Var}(\hat{G}_1[i, l_1]) \\
 &\quad + \mathbf{E}^2(\hat{G}_1[i, l_1])\mathbf{E}^2(\hat{G}_3[k, l_2])\mathbf{Var}(\hat{G}_2[j, l_1, l_2]) \\
 &\leq \sum_{l_1=1}^r \sum_{l_2=1}^r \frac{\|G_1\|_F^2 \|G_2\|_F^2 \|G_3\|_F^2}{(m_1 m_2)^3} + \frac{G_1^2[i, l_1] \|G_2\|_F^2 \|G_3\|_F^2}{(m_1 m_2)^2} + \frac{G_2^2[j, l_1, l_2] \|G_1\|_F^2 \|G_3\|_F^2}{(m_1 m_2)^2} \\
 &\quad + \frac{G_3^2[k, l_2] \|G_2\|_F^2 \|G_1\|_F^2}{(m_1 m_2)^2} + \frac{G_1^2[i, l_1] G_2^2[j, l_1, l_2] \|G_3\|_F^2}{m_1 m_2} + \frac{G_2^2[j, l_1, l_2] G_3^2[k, l_2] \|G_1\|_F^2}{m_1 m_2} + \frac{G_1^2[i, l_1] G_3^2[k, l_2] \|G_2\|_F^2}{m_1 m_2} \\
 &\leq r^2 G_{1a}^2 G_{2b}^2 G_{3c}^2 \left(\frac{1}{(m_1 m_2)^3} + \frac{3}{(m_1 m_2)^2} + \frac{3}{m_1 m_2} \right) \\
 &\leq 7r^2 \|G_1\|_F^2 \|G_2\|_F^2 \|G_3\|_F^2 \frac{1}{m_1 m_2}
 \end{aligned} \tag{29}$$

\square